



## Particle Deposition on a 300 mm Wafer Moving in the Opposite Direction of the Airflow in a Uni-directional Cleanroom

Yang-Cheng Shih<sup>1</sup>, Shih-Cheng Hu<sup>1\*</sup>, Chen-Wei Ku<sup>1</sup>, Reiyu Chein<sup>2</sup>

<sup>1</sup> National Taipei University of Technology, Taipei, Taiwan

<sup>2</sup> Natioanl Chung Hsing University, Taichung, Taiwan

### ABSTRACT

An investigation of the particle deposition velocity ( $v_d$ ) onto an upward moving 300 mm ( $d_w$ ) wafer in a cleanroom with a 0.3 m/s downward velocity ( $v_o$ ) was performed by the dynamic mesh model of FLUENT CFD code. The results show that the air simultaneously replenishes the vacant space induced by the movement of the wafer and new recirculation zones were formed around the wafer. These phenomena are apparently different from those of the wafer fixed (free-standing) in the flowing fluids. Compared with a free-standing wafer, the particle deposition velocity on a moving wafer was increased significantly. The deposition velocity increases with the increase of wafer moving velocity ( $v_b$ ). When the dimensionless moving velocity of the wafer  $V_b (= v_b/v_o)$  was 0.3, 1.0, and 3.3, the time averaged (over the dimensionless time  $\tau (= tv_o/d_w)$  from 0 to 1.0) particle deposition velocity of particles with diameter of 0.1  $\mu\text{m}$  was 11.4%, 20.8% and 37.8% greater than that of a free-standing wafer ( $v_{fs}$ ), respectively. In the computing range, the mean  $v_d$  can be estimated by an equation of  $v_d = v_{fs} (0.208 V_b^{1/2} + 1.0)$ .

**Keywords:** Particle deposition velocity; Dynamic Simulation; Computational Fluid Dynamics (CFD).

### INTRODUCTION

Deposition of particles on a surface is of great importance in many technological processes such as filtration, contamination control of microelectronic manufacture, control of surface fouling of microfluidic devices, and biofouling of artificial organs. Deposition of submicron and micron particles from aerosol flow on a wafer surface is of special interest in semiconductor manufacturing. Many studies on this aspect for a freestanding wafer have been reported theoretically (Liu and Ahn, 1987), numerically (Oh *et al.*, 1996; Schmidt *et al.*, 1997; Yoo *et al.*, 2004), and experimentally (Ye *et al.*, 1991; Opiolka *et al.*, 1994).

However, none of the existing studies focused on particle deposition when wafer is moving through the flow field. Actually, there are many scenarios that particles are even easier to deposit on wafer when the wafer is moving in a flow field. This takes place when wafers are in a sorter, in the up-loading/down-loading process or in a process tool. Therefore, effect of flow field on particle deposition by wafer moving deserves detail investigation.

In fluid dynamics, this problem belongs to a class of the moving boundary problems. From a relative velocity viewpoint, the moving body is traditionally and conveniently regarded as the stationary body in the flowing fluid, in which the relative velocity between the moving body and the fluid is considered. This is referred as “relative velocity method” in this paper. The most notable about the relative method is it neglects the fact that the fluid near the moving body must replenish the vacant space induced by the movement of the body. Actually, the dynamic problem of the moving body regarded as the stationary body in the flowing fluid is different from that of the body moving in the flowing fluid, especially the flow patterns around the moving object. Specifically, this study aims to investigate the variation of the flow and particle deposition velocity on a upward-moving circular plate in downward air and particle field and to compare with the result predicted by the relative method, in which the upward-moving circular plate is treated as a stationary body in a flowing fluid.

### NUMERICAL METHODS

Fig. 1 shows the schematic diagram for investigating effect of the moving wafer on particle deposition velocity in the flow. A wafer with length of  $d_w$  is set within the computational domain with height of  $h$  and width of  $W$ , respectively. The distance from the outlet of the domain to the wafer is  $h_1$ . The inlet velocity and particle concentration

\* Corresponding author. Tel.: +886-2-2771-2171 ext. 3588;  
Fax: +886-2-2731-4919  
E-mail address: f10870@ntut.edu.tw

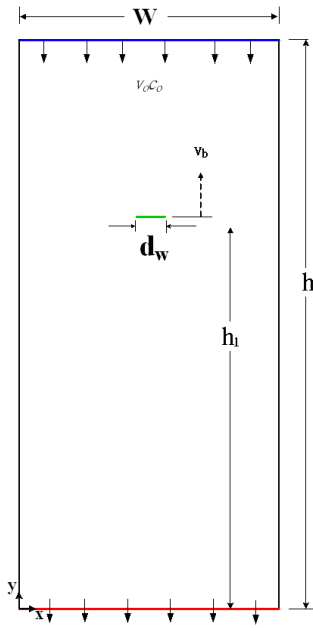


Fig. 1. Schematic of the computational domain.

of the fluid are constant and equal to  $v_o$  and  $c_o$ , respectively. Numerical calculations were performed with a laminar flow from the top. Particle inertial effect was neglected due to low inlet velocity. Initially ( $\tau = 0$ ), the wafer is stationary and fluid is flowing steadily. As the time  $\tau > 0$ , the wafer starts to move upward with a velocity  $v_b$ , which is opposite to the direction of the flowing fluid. The behavior of the wafer and fluid are then coupled, and the variation of the flow and particle concentration fields becomes time-dependent. As a result, the conservation equations for laminar flow are presented. In order to facilitate this problem, the following assumptions are made:

1. The fluid is air and the flow field is two-dimensional, incompressible and laminar.
2. The fluid properties are constant.
3. Particle concentration is uniform in the free stream.
4. The particle is completely absorbed as it impacts onto the wafer surface, i.e., zero particle concentration at the wafer surface.
5. The no-slip condition is held on the interfaces between the fluid and wall.

FLUENT provides comprehensive modeling capabilities for a wide range of incompressible and compressible, laminar and turbulent fluid flow problems. For all flows, FLUENT solves conservation equations for mass and momentum simultaneously. Based on the assumptions stated above, the equation for conservation of mass, or continuity equation can be written as follows:

$$\frac{\partial \rho}{\partial t} + \nabla \cdot (\rho \vec{v}) = S_m \quad (1)$$

Eq. (1) is the general form of the mass conservation equation and is valid for incompressible as well as compressible flows. The source  $S_m$  is the mass added to the

continuous phase from the dispersed second phase or any user-defined sources.

### Dynamic Meshes

The dynamic mesh model in FLUENT (2007) can be used to model flow field where the shape of the domain is time-dependent due to motion of the domain boundaries or moving object. The motion can be a prescribed or an un-prescribed motion and subsequent motion is determined based on the solution at the current time step. The update of the volume mesh is handled automatically by FLUENT at each time step based on the new positions of the boundaries.

The integral form of the conservation equation for a general scalar  $\phi$  over an arbitrary control volume with volume of  $V$  and moving boundary can be written as,

$$\frac{d}{dt} \int_V \rho \phi dV + \int_{\partial V} \rho \phi (\vec{u} - \vec{u}_g) \cdot d\vec{A} - \int_{\partial V} \Gamma \nabla \phi \cdot d\vec{A} = \int_V S_\phi dV \quad (2)$$

where  $\rho$  is the fluid density,  $\vec{u}$  is the flow velocity vector,  $\vec{u}_g$  is the grid velocity of the moving mesh,  $\Gamma$  is the diffusion coefficient, and  $S_\phi$  is the source term of  $\phi$ . Here  $\partial V$  is used to represent the boundary of the control volume. Using the first order backward difference formula, time derivative term in Eq. (2) can be written as,

$$\frac{d}{dt} \int_V \rho \phi dV = \lim_{\Delta t \rightarrow 0} \frac{(\rho \phi V)^{n+1} - (\rho \phi V)^n}{\Delta t} \quad (3)$$

where  $n$  and  $n + 1$  denote the respective quantity at the current and next time level. The  $(n + 1)^{\text{th}}$  time level volume  $V^{n+1}$  is computed from

$$V^{n+1} = V^n + \frac{dV}{dt} \Delta t \quad (4)$$

where  $dV/dt$  is the time derivative of the control volume. In order to satisfy the grid conservation law, the time derivative of the control volume is computed from

$$\frac{dV}{dt} = \int_{\partial V} \vec{u}_g \cdot d\vec{A} = \sum_j^{nf} \vec{u}_{g,j} \cdot \vec{A}_j \quad (5)$$

$$\vec{u}_{g,j} \cdot \vec{A}_j = \frac{\delta V_j}{\Delta t} \quad (6)$$

where  $\delta V_j$  is the volume swept out by the control volume face  $j$  over the time step  $\Delta t$ .

### Particle Deposition Velocity

The particle deposition velocity,  $v_d$ , to the wafer surface is determined by surface particle flux (number deposited per unit area and unit time) and particle concentration of downwash flow  $c_o$  as follows,

$$v_d = \frac{\sum J_i}{c_o} \quad (7)$$

Where  $J_i$  is the particle flux at wafer surface due to diffusion, sedimentation, inertia, or eddy impaction. For hydraulic smooth surfaces the particle flux due to diffusion is,

$$J_{diff} = -D \left. \frac{dc}{dy} \right|_{y=0} \quad (8)$$

Where  $D$  is the particle diffusion coefficient ( $m^2/s$ ),  $\left. \frac{dc}{dy} \right|_{y=0}$  is the particle concentration gradient (particle/ $m^4$ ) at

the wafer surface. In the present work, the first layer of grids were located at the distance of 10  $\mu m$  above the wafer surface (same as that of Oh. et al., (1996)), and the other 20 layers of grids were arranged to increase geometrically with geometric ratios less than 1.025.

Neglecting buoyancy effects, the particle flux due to sedimentation becomes

$$J_s = v_{ts} c_o \quad (9)$$

where  $v_{ts}$  is the drift velocity of particle due to sedimentation defined as

$$v_{ts} = \tau_p g \quad (10)$$

In Eq. (10),  $g$  is the gravitational acceleration,  $\tau_p$  is the particle relaxation time defined as,

$$\tau_p = \rho_p d_p^2 C_c / 18\mu \quad (11)$$

Where  $\rho_p$  is the density of particle,  $d_p$  the diameter of particle,  $C_c$  the slip factor of particle and  $\mu$  the viscosity of air.

The influence of inertia on particle deposition can be estimated using the critical Stokes number  $S_{tk} = v_o \tau_p / R$ , where  $R$  is the radius of the wafer. As the value of  $S_{tk}$  is far less than the critical Stokes number (Schmidt et al., 1997), the mass moment inertia can be neglected. The particle deposition due to eddy impaction is estimated to be negligible because the low Reynolds number flows are investigated in this study. The SIMPLE code modified for use in particle transport problem proposed by Stratmann and Whitby (1989) was used to solve the particle transport equation. The flow field was solved first using the Navier-Stokes equation. The resultant velocity field was then used as input into the particle transport equation. The averaged particle deposition velocity was calculated for the top side of the wafer.

## RESULTS AND DISCUSSION

### Model Verification for Free-Standing Case

As no experiment available, we firstly verify our model result with data from previous study to ensure our model result is reliable in free-standing case. The way of dynamic

mesh approach is composed of every free-standing case in each instant (time) over the moving period. We also compare our model result with the result of the “relative velocity method”. Fig. 2 shows the comparison of deposition velocity between the current CFD result and the available experimental and analytical data for a free-standing wafer. When  $dp \leq 0.1 \mu m$ , the deposition velocity increases significantly with the decrease in particle size while deposition velocity increases significantly with the increase in particle size when  $dp \geq 0.25 \mu m$ . As shown in Fig. 2, the current model results are in good agreement as compared with the experimental data of Opiolka et al. (1994). For  $dp = 0.1 \mu m$ , our predicted  $v_d$  value lies between the maximum and minimum values of the experiment data of Opiolka et al. (1994). In general, the current model data also show better agreement than that of Liu and Ahn’s analytical model (1987).

### The Transient Development of the Velocity Contours and Velocity Vectors

In this study, the downward air velocity was fixed at 0.3 m/s. The dimensionless wafer moving velocities ( $V_b$ ) considered were 0.3, 1.0, and 3.3. The dimensionless time step  $\Delta\tau$  is chosen to be 0.01. Fig. 3 shows the transient development of the velocity contours and velocity vectors around the wafer for the  $V_b = 0.3$  case. Initially with  $\tau = 0$  i.e., a free-standing scenario, the incoming air was impinging on the top surface and flow separations were observed. The separating point was located at the center of the top surface. Two recirculation zones around the wafer bottom surface can be identified apparently. As dimensionless time increases to  $\tau = 1$ , the wafer moves upward and pushes the incoming air near the top surface of the wafer, as shown in Fig. 3(b), and this air flows upward and the direction of air flow caused by wafer motion was the upward and downward flows become opposite in opposite to that of the downward inlet airflow. As a result, direction

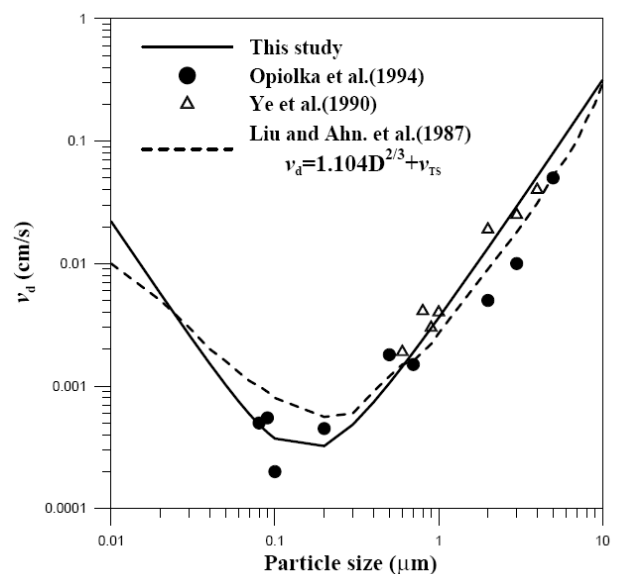
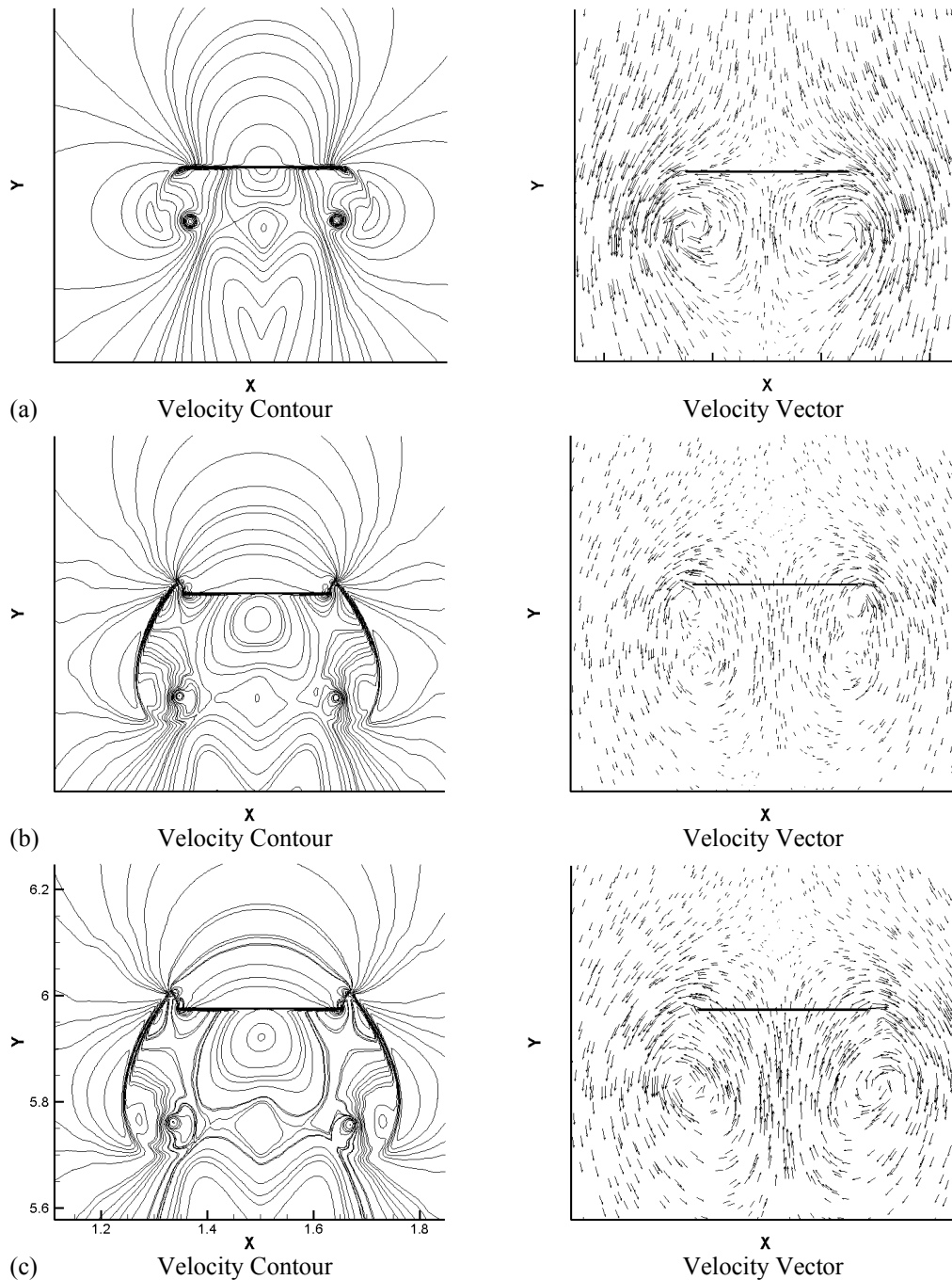


Fig. 2. Current CFD result vs. the available experimental and analytical data for a free-standing case.



**Fig. 3.** The transient development of velocity contours and velocity vectors around the wafer for  $V_b = 0.3$  case. (a)  $\tau = 0$ , (b)  $\tau = 0.1$ , (c)  $\tau = 0.25$

and create larger size of separation flows on the top surface. Therefore, the impinging flow patterns are not so obvious. Since the magnitude of the incoming air velocity was larger, the upward air motion mentioned above was deflected and became a downward flow in a short distance away from the wafer. No significant difference on the flow pattern was observed after  $\tau = 0.1$ .

Fig. 4 shows the transient development of velocity contours and velocity vectors around the wafer for  $V_b = 3.3$  case. Since the moving velocity of the wafer was greater than the  $V_b = 0.3$  case shown in Fig. 3, the variation of the

flow field near the wafer is more drastic. The upward velocity vectors near the top surface of the wafer in this case were apparently noted. As for the fluid near the bottom surface of the wafer, recirculation zones are formed around the corners of the bottom surface at first, and the recirculation zones grow larger. However, most of the fluid that fills the vacant space induced by the movement of the wafer was provided from the region behind the wafer, which is like the situation of the flow impinging on the bottom surface. No significant difference on the flow pattern was observed after  $\tau = 0.75$ .

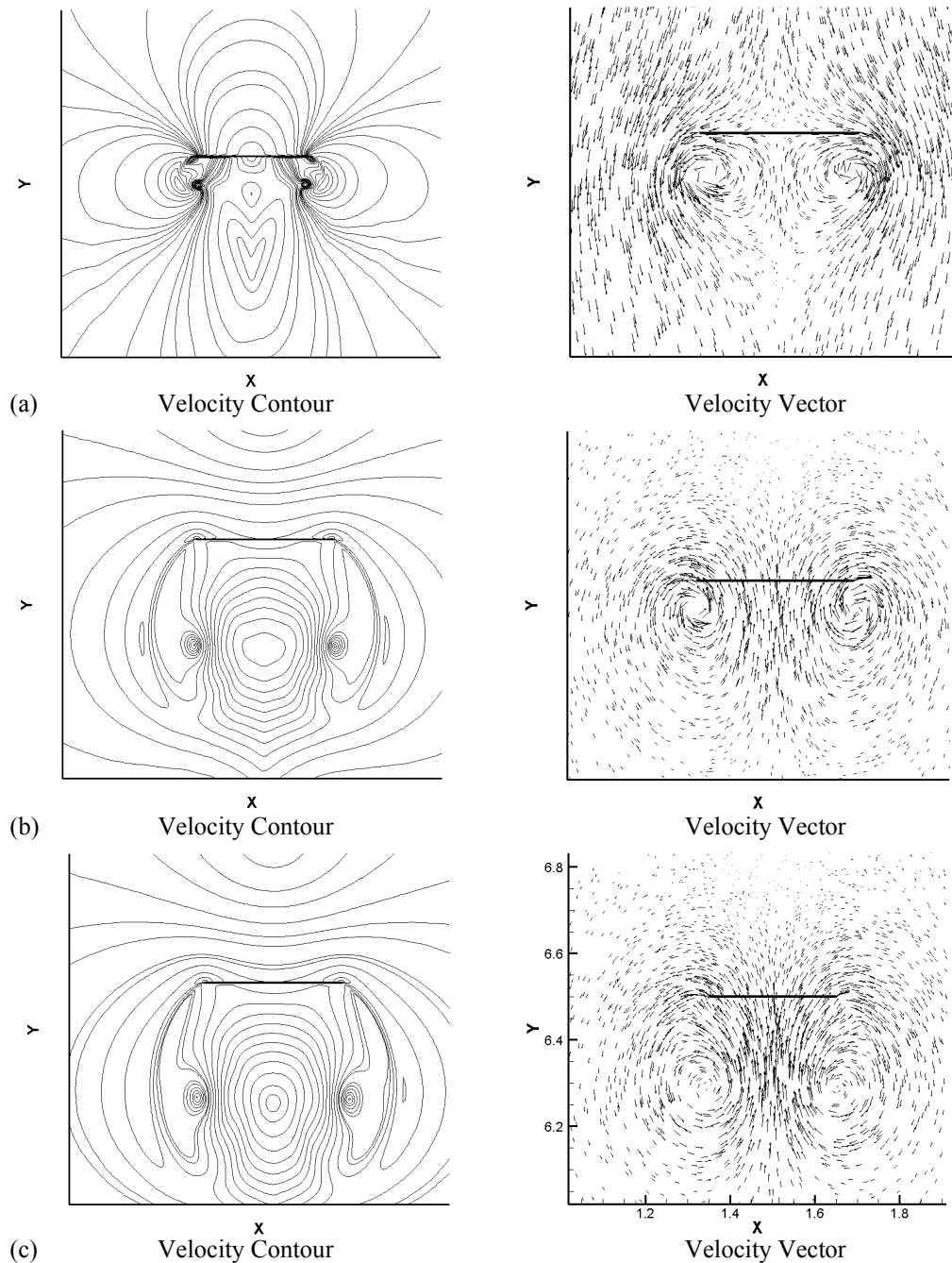


**Fig. 4.** The transient development of velocity contours and velocity vectors around the wafer for  $V_b = 3.3$  case. (a)  $\tau = 0$ , (b)  $\tau = 0.1$ , (c)  $\tau = 0.75$

From the above discussion, it is noted that the flow patterns around a moving wafer is apparently different from those of a wafer fixed in the flowing fluids i.e. a free-standing case.

**Variations of the Averaged Deposition Velocity on the Upper Surface of the Wafer**

Fig. 5. shows the particle concentration gradient  $\left(\frac{dc}{dy}\right)_{y=0}$  for the different moving velocity cases. The particle concentration boundary layer at the top surface of the wafer

becomes even thinner resulting high particle concentration gradient due to an upward move. As shown in Fig. 5, a greater value of the particle concentration gradient is observed for a high  $V_b$  case than that of a low  $V_b$  case.

Fig. 6. shows particle deposition velocity distribution between the current dynamic mesh method and the relative velocity method. Note that the particle deposition velocity under the relative velocity method is more greatly than that of dynamic mesh method for particles less than  $0.1 \mu\text{m}$ . This is because that the relative velocity method overlooks the influences of flow field by the moving object. In the dynamic mesh method, the wafer moving upward, and the

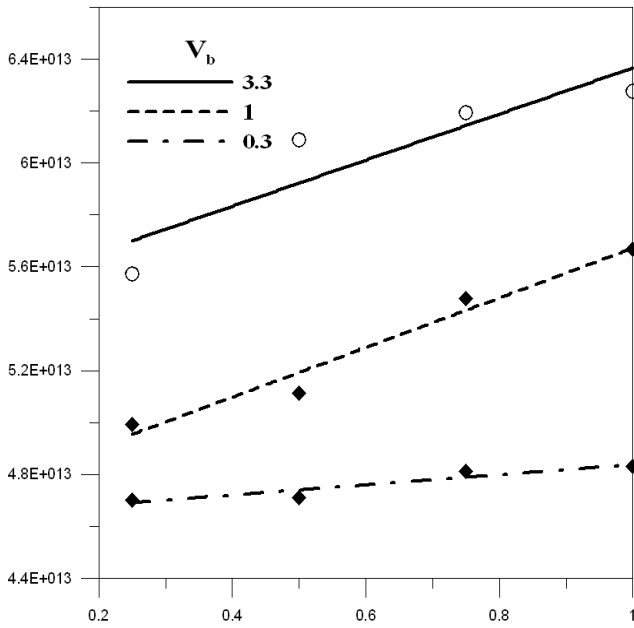


**Fig. 5.** Particle concentration gradient near the wafer surface for the cases  $V_b = 0.3, 1.0,$  and  $3.3$ .

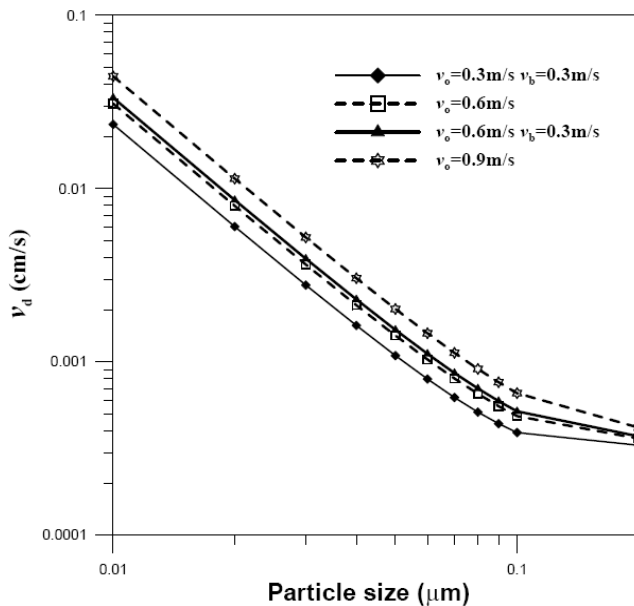


**Fig. 6.** A comparison of deposition velocity between dynamic mesh method (in solid lines) and relative velocity method (in broken lines).

direction of this motion is opposite to that of the inlet fluid, the momentum predicted by the dynamic mesh method is smaller than that predicted by relative velocity method. Note that the relative velocity method predicts a slightly greater value of  $v_d$  than that by dynamic mesh method, especially for high  $v_b$  cases.

Several different moving velocities of the wafer are taken into consideration in determining the relationship among the variables of the particle deposition velocity  $v_d$ , moving velocity of the wafer  $V_b$  for the duration of the transient development. The relationship between the

particle deposition velocity  $v_d$  and  $v_b$  can be correlated as Eq. (12) by dynamic mesh method and Eq. (13) by relative velocity method:

$$v_d/v_{fs} = 0.208 V_b^{1/2} + 1.0 \quad (12)$$

$$v_d/v_{fs} = 0.233 V_b^{1/2} + 1.0 \quad (13)$$

Where  $v_{fs}$  indicates the deposition velocity of a free-standing plate under a downward velocity of 0.3 m/s. When the dimensionless moving velocity of the wafer  $V_b$  was 0.3, 1.0, and 3.3, the particle deposition velocity of particles with diameter of 0.1  $\mu\text{m}$  is 11.4%, 20.8% and 37.8% greater than that of a free-standing wafer, respectively.

### CONCLUSION

The particle deposition velocity of a wafer moving with direction opposite to a flowing fluid is studied numerically by the dynamic mesh method of CFD techniques. Based on the results and discussion, some conclusions are summarized as follows:

1. The flow pattern around a moving wafer is apparently different from those of a wafer fixed in the flowing fluid, i.e., a free-standing case. The wafer moving upward cause the particle concentration gradient increase, resulting in a greater value of particle deposition velocity. These phenomena are apparently different from those of the wafer fixed in the flowing fluid.
2. The relative method velocity predicts a greater value of particle deposition velocity than that by the dynamic mesh method proposed in the present study.

### REFERENCES

Fluent 6.3 User's Guide (2007). Fluent Inc., Lebanon, U.S.A.  
 Liu, B. Y. H., and Ahn, K. H. (1987). Particle Deposition on Semiconductor Wafers. *Aerosol Sci. Technol.* 6: 215–224.  
 Oh, M.D., Yoo, K.H. and Myong, H.K. (1996). Numerical Analysis of Particle onto Horizontal Freestanding Wafer Surfaces Heated or Cooled. *Aerosol Sci. Technol.* 25: 141–156.  
 Opiolka, S., Schmidt, F. and Fissan, H. (1994). Combined Effect of Electrophoresis and Thermophoresis on Particle Deposition onto Flat Surface. *J. Aerosol Sci.* 25: 665–671.  
 Schmidt, F., Gartz, K. and Fissan, H. (1997). Turbulent Particle Deposition on a Horizontal Circular Plate. *J. Aerosol Sci.* 28: 973–984.  
 Stratmann, F. and Whitby, E.R. (1989). Numerical Solution of. Aerosol Dynamics for Simultaneous Convection, Diffusion and External Forces. *J. Aerosol Sci.* 20:437–440.  
 Ye, Y., Pui, D.Y.H., Liu, B.Y.H., Opiolka, S., Blumhorst,

S. and Fissan, H. (1991). Thermophoretic Effect of Particle Deposition on a Free-standing Semiconductor Wafer in a Cleanroom. *J. Aerosol Sci.* 22: 63–72.

Yoo, K.H., and Oh, M.D. (2004). Numerical Analysis on Flow Field and Particle Deposition on a Heated

Spinning Disk. *J. Aerosol Sci.* 36: 235–246.

*Received for review, August 24, 2009*

*Accepted, February 17, 2010*